DFT Study on the Effect of Aluminum Atom Distribution in Zn-exchanged MFI zeolites for Methane C-H Bond Activation

by

Sandra Cecilia Albarracin Suazo

A thesis submitted in partial fulfillment of the requirements for the degree of

MASTER OF SCIENCE
in
CHEMICAL ENGINEERING

UNIVERSITY OF PUERTO RICO
MAYAGÜEZ CAMPUS
2018

Approved by:

Yomaira J. Pagán-Torres, PhD President, Graduate Committee	Date
María C. Curet-Arana, PhD Member, Graduate Committee	Date
Nelson Cardona Martínez, PhD Member, Graduate Committee	Date
María M. Martínez Iñesta, Ph.D. Member, Graduate Committee	Date
Aldo Acevedo Rullán, Ph.D. Chair of the Department	Date
Juan C. Neco Valle, MS Graduate School Representative	Date

Abstract

The direct conversion of methane to useful chemicals is economically attractive owing to the vast availability of natural gas resources. Nevertheless, a fundamental limitation is the chemical inertness and stability of the C-H bond of the CH_4 molecule. Recently, metal-ion exchanged aluminosilicates (i.e., Zn-MFI,) have been shown to be active in the C-H bond activation of methane, however elucidation of the effect of the Al atom array within the rings of MFI on the formation of the active site remains unknown. In this work, we use Density Functional Theory (DFT) with specific treatment of Van der Waals forces to systematically analyze the effect of Al atom distribution within the α-ring of Zn-MFI on the activation of methane. In these studies, we have: (1) identified the preferred site for Zn^{2+} exchange in the α-ring of MFI as a function of Al atom arrangement, (2) developed a relative energy diagram for C-H bond activation in CH_4 as a function of the Al atom array in the α-ring of Zn-MFI, and (3) developed correlations based on electrostatic and electron transfer interactions between CH_4, the Zn metal center, and the MFI α-ring. Among the clusters analyzed, we determined that the lowest energy barrier for C-H bond activation of CH_4 is obtained for the Zn-MFI-5 configuration in which the Al atoms are located at the T8 and T5 sites of the α-ring. Our work unravels that Al atoms distribution produces a variation in the energy barrier in the detachment of a hydrogen atom from methane. Furthermore, the most energetically stable Al configuration does not yield the lowest energy barrier for methane activation.

Resumen

La conversión directa de metano a productos químicos de impacto económico e industrial ha tomado importancia en los últimos años debido a la gran disponibilidad de recursos de gas natural. Sin embargo, la limitación principal es la estabilidad del enlace C-H de la molécula CH_4. Recientemente, se ha demostrado que las zeolitas como Chabasita, MFI o Faujasita intercambiados con iones metálicos son idóneos para la activación de metano. Sin embargo, el efecto que tiene la configuración de los átomos de Al en el momento de realizar la síntesis en el sitio activo en la zeolita MFI sigue siendo desconocido. En este trabajo, usamos la teoría del funcional de la densidad (o DFT, por sus siglas en inglés, Density functional theory) con un tratamiento específico de las fuerzas de Van der Waals para analizar sistemáticamente el efecto de la distribución de los átomos de Al dentro del anillo α de Zn-MFI sobre la activación del metano. En estos estudios, hemos: (1) identificado el sitio energéticamente más favorable para el intercambio del átomo de Zn en el anillo α en función de la configuración de los átomos de Al, (2) desarrollamos un diagrama de energía para el rompimiento del enlace C-H de CH_4 como función de la distribución de los átomos de Al en el anillo α de Zn-MFI, y (3) desarrollamos correlaciones basadas en interacciones electrostáticas y de transferencia de electrones entre CH_4, el centro metálico (Zn) y el anillo α de MFI. Entre las configuraciones estudiadas, determinamos que la barrera energética más favorable para la activación del enlace C-H de CH_4 se obtiene para la configuración de Zn-MFI -5 en la que los átomos de Al están ubicados en los sitios **T8** y **T5** del anillo α. Nuestro trabajo demuestra que la distribución de los átomos de Al produce una variación en la barrera de energía en la extracción de un

átomo de hidrógeno del metano. Además, la configuración de Al más estable energéticamente no produce la barrera de energía más baja para la activación de metano.

Acknowledgments

I owe an unimaginable thanks to my family, my mother, Maria Ana Suazo; my brother, Erwin R. Suazo; my nephew Joaquin and his persistent smile; my friend, Lady Rodriguez, who I love like a sister and Manny de Jesus without whose support I would not have traveled so far.

I want to thank my research partners Brian Montejo-Valencia and Dr. Paul Meza Morales for their teachings and their patience. I want to show my gratitude to my advisor's Dr. Yomaira Pagan-Torres and Dr. María C. Curet-Arana, whose continuous supports, guidance and encouragements made all the work presented here possible. Finally, and not least, my most sincere gratitude to Dr. María M. Martínez Iñesta and Dr Nelson Cardona Martínez for their feedback and collaboration in my research work.

To God, my mom
Maria Ana Suazo,
my brother
Erwin Suazo,
My boyfriend
Manny X. de Jesus
for their love,
motivation
and guidance.

Wang, B.; Albarracín-Suazo, S.; Pagán-Torres, Y.; Nikolla, E., Advances in methane conversion processes. *Catalysis Today* **2017**, 285, 147-158.

This article is available online at https://doi.org/10.1016/j.cattod.2017.01.023.

Table of Contents

List of Tables

List of Figures

Chapter 1. Introduction

Methane is the simplest alkane hydrocarbon that exists in the earth's crust, it occurs naturally as the final product of the anaerobic putrefaction of plants.[1] Methane is an abundant source of carbon primarily found in natural gas. According to the international energy agency (EIA), the production of natural gas has had an exponential growth since 2007 as shown in Fig 1.1 with the advent of fracking.[2]

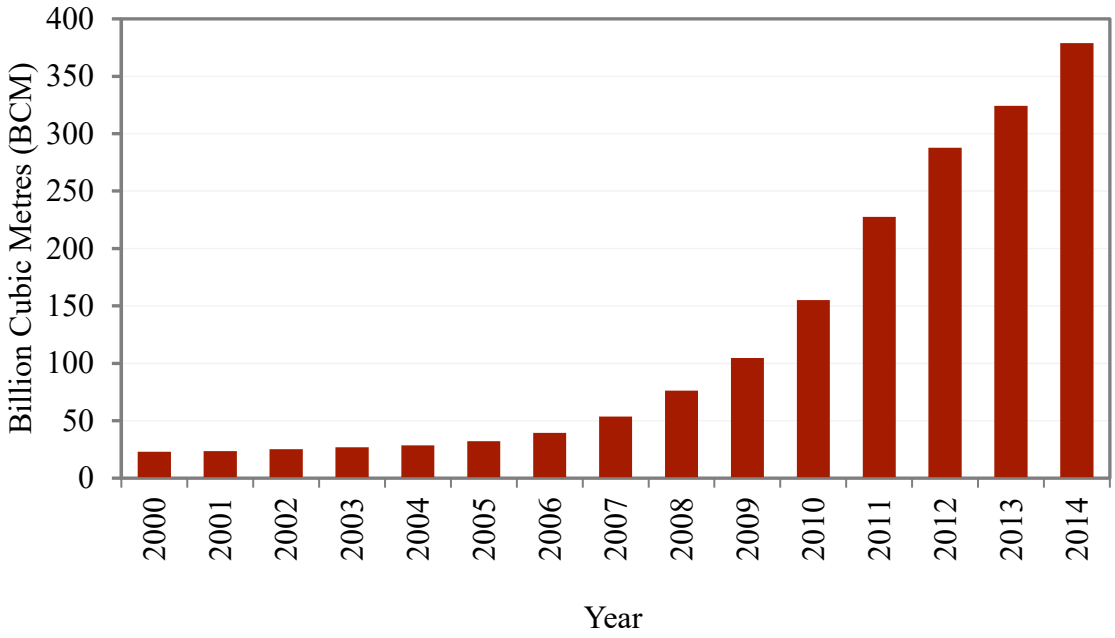

Fig 1.1. Shale gas production from 2000 to 2014 in USA. Sourches: EIA derived from state administrative data collected by DrillingInfo Inc.[2]

The motivation of this project is the direct conversion of methane in value-added compounds such as methanol and acetic acid. However, methane has a high dissociation energy of 440 kJ/mol, and the reactivity of the methyl radicals formed imposes difficulties on the selectivity of reactions.[3] Recently, the MFI zeolite has been demonstrated to activate methane at low temperatures when it is exchanged with zinc cation (Zn-MFI).[4] Therefore, experimental[4-8] and

theoretical[9-11] studies have focused efforts on understanding the mechanism of H atom abstraction from methane within the pore of this zeolite. For instance, by using 1H and 13C NMR techniques, Pirogov and co-workers demonstrated that upon methane activation over Zn-MFI, a hydroxyl group is formed in the zeolite.[5] The studies demonstrated that these hydroxyl groups are stable and cause a reduction of the catalytic activity. Previous studies have also reported that the Brønsted acidity of the MFI zeolite varies depending on the distribution of the aluminum (Al) atoms within the framework. Moreover, the distribution of Al atoms in the T-sites of the zeolites can affect the energy barrier for methane activation.[12] Thus, the catalytic activity can be compromised depending on this distribution, and this can result in low conversion rates.[13-14] Studies have aimed to analyze the Al distribution in MFI. For instance, Sauer and coworkers combined high-resolution 27Al-NMR spectroscopy with density functional theory (DFT) / molecular mechanics calculations, and they established which of the 13 distinguishable T-sites of MFI are occupied by Al-atoms.[15-16] Furthermore, Tatsumi and coworkers were able to control the location of Al-atoms on MFI by using different organic molecules during the synthesis of the zeolite. For instance, when tetrapropylammonium cations were used, Al-atoms are primarily located at the intersection of the zeolite channels.[17]

Recently, Norskov and coworkers conducted DFT studies to analyze the effect of Al positions in Cu-MOR for the oxidation of methane to methanol. These studies demonstrated that the energy barrier for methane activation varies with the Al-atom positions in the 12 membered-ring of MOR. Adsorption energies ranged from 43 to 65 kJ/mol and activation energies from 63 to 124 kJ/mol, depending on the position of the Al atoms within the ring.[18] To our knowledge, a similar study on MFI, which has been more widely used for methane activation still lacks in the literature.

For this research work we hypothesize that for metal-exchanged MFI zeolites the arrangement of Al atoms within the ring can have a direct effect in the energy barrier of the detachment of the hydrogen atom from methane.

The hypothesis will be probed by (1) identifying the preferred site for Zn^{2+} exchange in the α-ring of MFI as a function of Al atom arrangement, (2) developing a relative energy diagram for C-H bond activation in CH_4 as a function of the Al atom array in the α-ring of Zn-MFI, and (3) developing correlations based on electrostatic and electron transfer interactions between CH_4, the Zn metal center, and the MFI α-ring.

References

1. Stauffer, E.; Dolan, J. A.; Newman, R. *Fire Debris Analysis*; Elsevier Science, **2007**.
2. Information, U. S. E. A. Review of Emerging Resources: U.S. Shale Gas and Shale Oil Plays https://www.eia.gov/energyexplained/index.php?page=natural_gas_where (accessed May 20, 2018).
3. Kolyagin, Y. G.; Ivanova, I. I.; Ordomsky, V. V.; Gedeon, A.; Pirogov, Y. A., Methane Activation over Zn-Modified MFI Zeolite: NMR Evidence for Zn−Methyl Surface Species Formation. *The Journal of Physical Chemistry C* **2008**, *112*, 20065-20069.
4. Gabrienko, A. A.; Arzumanov, S. S.; Luzgin, M. V.; Stepanov, A. G.; Parmon, V. N., Methane Activation on Zn^{2+}-Exchanged ZSM-5 Zeolites. The Effect of Molecular Oxygen Addition. *The Journal of Physical Chemistry C* **2015**, *119*, 24910-24918.
5. Kolyagin, Y. G.; Ivanova, I. I.; Pirogov, Y. A., 1H and 13C MAS NMR Studies of Light Alkanes Activation over MFI Zeolite Modified by Zn Vapour. *Solid State Nuclear Magnetic Resonance* **2009**, *35*, 104-112.
6. Arzumanov, S. S.; Gabrienko, A. A.; Freude, D.; Stepanov, A. G., Competitive Pathways of Methane Activation on Zn^{2+}-Modified ZSM-5 Zeolite: H/D Hydrogen Exchange with Bronsted Acid Sites Versus Dissociative Adsorption to Form Zn-Methyl Species. *Catal Sci Technol* **2016**, *6*, 6381-6388.
7. Kolyagin, Y. G.; Ivanova, I. I.; Ordomsky, V. V.; Gedeon, A.; Pirogov, Y. A., Methane Activation over Zn-Modified MFI Zeolite: Nmr Evidence for Zn−Methyl Surface Species Formation. *The Journal of Physical Chemistry C* **2008**, *112*, 20065-20069.
8. Xu, J.; Zheng, A.; Wang, X.; Qi, G.; Su, J.; Du, J.; Gan, Z.; Wu, J.; Wang, W.; Deng, F., Room Temperature Activation of Methane over Zn Modified H-Zsm-5 Zeolites: Insight from Solid-State Nmr and Theoretical Calculations. *Chemical Science* **2012**, *3*, 2932-2940.
9. Blaszkowski, S. R.; Nascimento, M. A. C.; van Santen, R. A., Activation of C−H and C−C Bonds by an Acidic Zeolite: A Density Functional Study. *The Journal of Physical Chemistry* **1996**, *100*, 3463-3472.
10. Oda, A.; Torigoe, H.; Itadani, A.; Ohkubo, T.; Yumura, T.; Kobayashi, H.; Kuroda, Y., Mechanism of Ch4 Activation on a Monomeric Zn2+-Ion Exchanged in MFI-Type Zeolite with a Specific Al Arrangement: Similarity to the Activation Site for H2. *The Journal of Physical Chemistry C* **2013**, *117*, 19525-19534.
11. Pidko, E. A.; van Santen, R. A., Activation of Light Alkanes over Zinc Species Stabilized in Zsm-5 Zeolite: A Comprehensive Dft Study. *The Journal of Physical Chemistry C* **2007**, *111*, 2643-2655.
12. Gounder, R.; Iglesia, E., Catalytic Consequences of Spatial Constraints and Acid Site Location for Monomolecular Alkane Activation on Zeolites. *J Am Chem Soc* **2009**, *131*, 1958-1971.
13. Sazama, P.; Dědeček, J.; Gábová, V.; Wichterlová, B.; Spoto, G.; Bordiga, S., Effect of Aluminium Distribution in the Framework of Zsm-5 on Hydrocarbon Transformation. Cracking of 1-Butene. *J Catal* **2008**, *254*, 180-189.
14. Song, C., et al., Cooperativity of Adjacent Brønsted Acid Sites in MFI Zeolite Channel Leads to Enhanced Polarization and Cracking of Alkanes. *J Catal* **2017**, *349*, 163-174.

15. Sklenak, S.; Dedecek, J.; Li, C.; Wichterlova, B.; Gabova, V.; Sierka, M.; Sauer, J., Aluminium Siting in the Zsm-5 Framework by Combination of High Resolution 27al Nmr and Dft/Mm Calculations. *Phys Chem Chem Phys* **2009**, *11*, 1237-1247.
16. Dedecek, J.; Balgová, V.; Pashkova, V.; Klein, P.; Wichterlová, B., Synthesis of Zsm-5 Zeolites with Defined Distribution of Al Atoms in the Framework and Multinuclear Mas Nmr Analysis of the Control of Al Distribution. *Chemistry of Materials* **2012**, *24*, 3231-3239.
17. Yokoi, T.; Mochizuki, H.; Namba, S.; Kondo, J. N.; Tatsumi, T., Control of the Al Distribution in the Framework of Zsm-5 Zeolite and Its Evaluation by Solid-State Nmr Technique and Catalytic Properties. *The Journal of Physical Chemistry C* **2015**, *119*, 15303-15315.
18. Zhao, Z.-J.; Kulkarni, A.; Vilella, L.; Nørskov, J. K.; Studt, F., Theoretical Insights into the Selective Oxidation of Methane to Methanol in Copper-Exchanged Mordenite. *Acs Catal* **2016**, *6*, 3760-3766.

Chapter 2. Background

2.1 Methane conversion processes

The increased methane (CH_4) availability has sparked interest in using methane as a raw material to produce chemicals, such as methanol (CH_3OH).[1] According to the U.S. Energy Information Administration (EIA), coalbed methane reserve has reached the 12.5 billion cubic feet in the United States.[2] It is thus expected that in a near future, methane will be a source for the production of hydrocarbons.[3] Currently, however, methane is mainly used in industry for the production of syngas, at temperatures higher than 973 K. Syngas is then catalytically converted into chemicals, such as hydrocarbons or alcohols. The direct conversion of methane to value-added products is still a major challenge in catalysis. Methane has a high dissociation energy of 439 kJ/mol, and the reactivity of the methyl radicals formed imposes difficulties on the selectivity of reactions.[4]

The development of processes for the partial oxidation of methane to methanol through a low-temperature direct route from an inexpensive and abundant feedstock is a long-standing challenge, stimulated by the numerous applications of the chemical as a solvent and a precursor for the production of commodity chemicals, such as formaldehyde, methyl *tert*-butyl ether, acetic acid, chloromethanes, methyl methacrylate.[5,6] Current industrial methanol synthesis from methane involves a high-temperature and energy-intensive process involving the formation of synthesis gas by autothermal reforming, followed by the conversion of the synthesis gas to methanol over $Cu/ZnO/Al_2O_3$ catalysts.[7,8] Although the current industrial process produces methanol in high yields it requires high temperatures and pressures at various stages, in addition to large-capital intensive reforming facilities,[7,8] which limit the implementation of this technology in remote and

inconveniently located untapped natural gas reserves.[7] Therefore significant interest in the development of direct low-temperature methane to methanol processes, that circumvent the production of synthesis gas, has emerged to exploit the transformation of abundant and remotely located sources of natural gas.[9] Inspired by the remarkable activity and selectivity of methanotrophic bacteria to convert methane at mild reaction conditions over methane monooxygenase enzymes (MMO),[10-13] transition metal-exchanged zeolites, with active sites analogous to those in MMO have been studied as reactive materials for the activation of the highly stable C-H bond (438.8 kJ mol^{-1}) of methane at low temperatures (< 250 °C).[14-16] The active site of these enzymes for methane oxidation has been elucidated as bis(μ-oxo)diiron complexes in soluble methane monooxygenase (sMMO) and as bis(μ-oxo)dicopper complexes in particulate methane monooxygenase (pMMO).[10, 17]

2.2 Fe- and Cu-exchanged MFI and MOR zeolites for methane conversion

The first efforts in developing inorganic heterogeneous materials for the oxidation of methane to methanol, with active sites similar to sMMO enzymes, were Fe-ZSM-5 zeolites activated with nitrous oxide (N_2O).[18-19] The N_2O assisted in the formation of an active bridging Fe-oxo complex for hydrogen atom abstraction from methane.[18-19] A bis(μ-oxo)diiron cluster similar to the active center in sMMO was elucidated by in-situ Mossbauer spectroscopy studies of Fe-exchanged ZSM-5.[20] In addition to Fe-exchanged zeolites, Cu-exchanged ZSM-5 has received considerable interest for methane oxidation to methanol. The elucidation of the active Cu species in ZSM-5 has been subject of numerous spectroscopic and theoretical studies.[21-23] Pioneering work on Cu-exchanged ZSM-5 was conducted by Groothaert et al., which demonstrated the partial oxidation of methane by a stepwise and stoichiometric reaction with molecular oxygen at low

temperatures.[21] A bis(μ-oxo)dicopper complex has been proposed as the active site by a number of studies,[21-24] however, some have identified the site by resonance Raman spectroscopy and DFT studies as a bent mono-(μ-oxo)dicopper cluster located at the intersection of two 10-membered rings.[25-26]

Although a number of Cu-oxo species in ZSM-5 have been identified as active sites for methane oxidation to methanol, most suggested species are comprised of more than one Cu atom.[24] In a recent work, a comprehensive theoretical study based on DFT and *ab initio* thermodynamic analysis was conducted by Li et al. on the structure, stability, and reaction mechanism of extra-framework Cu complexes in ZSM-5 (e.g., bi- and trinuclear Cu-oxo species) as a function of activation and reaction conditions.[27] The formation of extra-framework trinuclear Cu-oxo species in ZSM-5, $[Cu_3(\mu\text{-}O)_3]^{2+}$, was shown to take place under oxygen-rich environments at high temperatures, whereas the formation of binuclear Cu species, $[Cu(\mu\text{-}O)Cu]^{2+}$, are formed and stabilized in low oxygen partial pressure environments during catalyst activation. Theoretical studies indicated that both the binuclear Cu complex $[Cu(\mu\text{-}O)Cu]^{2+}$ and trinuclear Cu-complex $[Cu_3(\mu\text{-}O)_3]^{2+}$ were reactive for C-H bond activation, however, the trinuclear Cu-complex exhibited the lowest energy pathway as shown in Fig. 2.1.[27] It is important to note that after reaction, the trinuclear Cu-species $[Cu_3(\mu\text{-}O)_3]^{2+}$ was transformed to a partially reduced Cu complex, $[Cu_3(\mu\text{-}O)_2]^{2+}$, hence regeneration of the active site was essential for the next methane conversion cycle.[27]

Markovits et al. studied the effect of the location and distribution of Al sites in ZSM-5 on the formation of Cu-oxo species to understand the structure and chemical environment required for the stabilization of these active sites.[28] A number of Cu-ZSM-5 materials with high

concentrations of Al pairs and different loadings of Cu were synthesized and studied in the stepwise oxidation of methane to methanol. From a combination of IR spectroscopy, extended X-ray absorption fine structure (EXAFS) studies, and DFT computed geometrical parameters of Cu-oxo complexes,[27] the authors proposed structures for the Cu-oxo complexes in ZSM-5. Trinuclear Cu-oxo complexes $[Cu_3(\mu\text{-}O)_3]^{2+}$ bonded to two paired framework Al as active sites for Cu-exchanged ZSM-5 for Cu/Al ratios of 0.2 to 0.5 and a combination of Cu monomers and dimers $[Cu_2(\mu\text{-}O)]^{2+}$ for Cu/Al ratios below 0.2 were proposed.[28] The highest yield obtained for methane oxidation was of 89 μmol g_{cat}^{-1} over Cu-ZSM-5 catalyst with Cu/Al ratios of approximately 0.5. Although the synthesized zeolites by Markovits et al. displayed high yields for methane oxidation, it should be noted that only 50% of the sites were active.[28] In addition to the nature of the extra-framework Cu-oxo cluster, it was concluded that the size and shape of the zeolite environment where the embedded Cu cluster is localized impacts its reactivity in methane conversion.

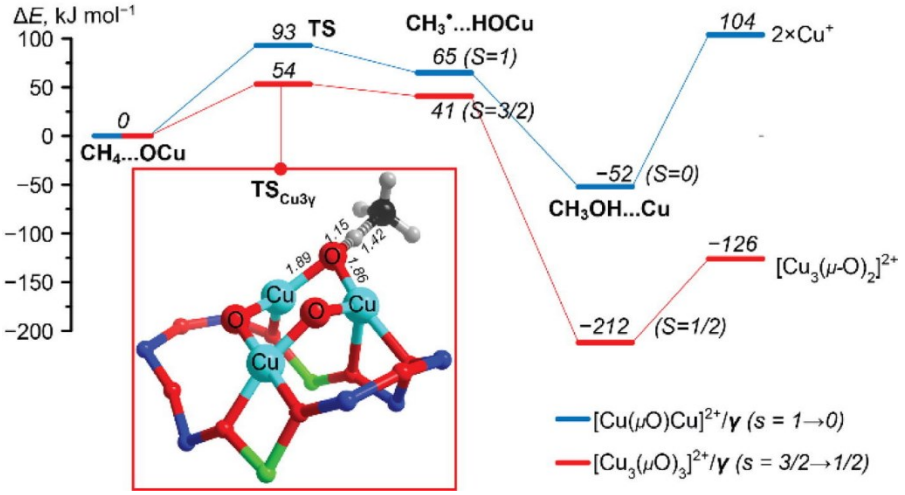

Fig 2.1 Minimum reaction energy paths for methane conversion to methanol over binuclear Cu-oxo complex, [Cu(μ-O)Cu]2+, and the trinuclear Cu-oxo complex, [Cu3(μ-O)3]2+, in Cu-ZSM-5. Reprinted from ref 27, Copyright 2018, with permission from Elsevier.

Interestingly, Cu-oxo species in other zeolite frameworks such as mordenite (MOR) have demonstrated higher methanol yields for the oxidation of methane compared to Cu-exchanged H-ZSM-5 materials.[29] Vanelderen et al. conducted detailed Raman spectroscopy studies to elucidate the structure of Cu active sites in MOR.[30] The sites were identified as two different $[Cu_2O]^{2+}$ clusters located in the 8-membered ring (MR) side pockets of MOR.[30] Depending on the framework environment in which the $[Cu_2O]^{2+}$ sites were located, differences in methane oxidation reactivity were observed.[30] Besides $[Cu_2O]^{2+}$ clusters being identified as active species for methane conversion, trinuclear Cu-oxo species in MOR have recently demonstrated high reactivity for C-H bond activation.[29] The combination of in-situ X-ray absorption spectroscopy (XAS) and DFT calculations determined the active site as a trinuclear Cu-oxo cluster, $[Cu_3(\mu\text{-}O)_3]^{2+}$, bonded to two Al atoms located at the entrance of the 8-MR side pocket. The barrier for methane C-H bond activation of 74 kJ mol^{-1} was determined for the $[Cu_3(\mu\text{-}O)_3]^{2+}$ complex in MOR, comparable to the 78 kJ mol^{-1} barrier obtained for methane C-H bond activation over the binuclear $[Cu(\mu\text{-}O)Cu]^{2+}$ complex in ZSM-5.[29] On the other hand, Zhao et al. performed DFT studies on the formation and reactivity of extra-framework $[CuOCu]^{2+}$ and $[CuOOCu]^{2+}$ complexes as active centers in MOR for methane to methanol oxidation.[31] Results suggested that the $[CuOCu]^{2+}$ complex is the most stable to be formed in MOR and is also the most reactive in activating methane between the two moieties studied.[31]

Grundner et al. optimized the synthesis of Cu-exchanged MOR zeolites for the deposition of a high number of uniform trinuclear Cu complexes in H-MOR resembling the structure and reactivity of active sites in pMMO, while minimizing the formation of Cu spectators.[32] Heterogeneous speciation of Cu (e.g., tri-, di-, and mononuclear species) in MOR was shown to be affected by synthesis conditions, including solution pH and the cation in the parent zeolite. The

presence of Na^+ and other alkaline earth cations in the 8-MR side pockets were shown to hinder the formation of trinuclear Cu-oxo species. For Cu-exchanged H-MOR a stoichiometry of 3:1 Cu to activated methane confirmed that all extra-framework trinuclear Cu-oxo species formed were reactive for methane conversion. Despite the fact that a similar trinuclear Cu-oxo complex $[Cu_3(\mu\text{-}O)_3]^{2+}$ has been identified in both Cu-H-MOR and Cu-H-ZSM-5, the methane oxidation activity of Cu-H-ZSM-5 is almost 50% that of Cu-H-MOR.[28] It has been hypothesized that in H-ZMS-5 the Cu-oxo species are located in more than one environment and in some cases the $[Cu_3(\mu\text{-}O)_3]^{2+}$ is in a less constrained local environment exhibiting higher free energy barrier for C-H bond activation. Whereas in Cu-H-MOR, most of the $[Cu_3(\mu\text{-}O)_3]^{2+}$ complexes are stabilized in a highly constrained local environment in the 8-MR side pockets with a lower free energy barrier.[28-30]

2.3 Different zeolite topologies for methane conversion

Besides MFI and MOR, other zeolite topologies such as ferrierite,[21] Beta,[21] Y,[21] SSZ-13,[33] SSZ-16,[33] SSZ-39,[33], and SAPO-34[33] exchanged with Cu have shown methane oxidation activity to methanol. Smeets et al. demonstrated that Cu-Beta and Cu-ferrierite are reactive materials containing active copper species different to those identified in Cu-MOR and Cu-ZSM-5 zeolite[31]. Cu-exchanged in 8-MR small pore zeolites (e.g., Cu-SSZ-13, Cu-SSZ-16, Cu-SSZ-39, Cu-SAPO-34) synthesized by Wulfers et al. produced higher methanol per Cu atom yields in comparison to Cu-ZSM-5 and Cu-MOR [33]. Kulkarni et al. investigated the active site in Cu-SSZ-13 through DFT calculations. A mono-copper species $[Cu^{II}OH]^+$ was proposed based on their results and previously reported spectroscopic and experimental studies [34]. Furthermore, the need of water for methanol extraction and the effect of the Si/Al ratio of Cu-SSZ-13 on reactivity were investigated by *ab-initio* molecular dynamics simulations. The presence of extra water molecules for the extraction of intermediate species was shown to hydrate the Cu atom, causing the detachment of a [Cu-

$2(H_2O)\text{-}CH_3]^+$ species from the framework Al.[34] The authors proposed that the formation of the mobile hydrated-Cu species gave a possible alternative route for methanol extraction through a more favorable energy path.

2.4 Metal ion-exchanged ZSM-5 for methane conversion

Ni-ZMS-5,[35] Co-ZSM-5,[36-37] and Zn-ZSM-5[38-39] have also shown reactivity in the oxidation of methane to methanol with molecular oxygen. Shan et al. reported that Ni-ZSM-5 converts methane with molecular oxygen to a mixture comprised of methanol, formaldehyde, and ethylene glycol at 150 °C and atmospheric pressure.[35] The total oxygenated product yield was of 14.9 μmol g_{cat}^{-1}.[35] Based on UV-vis, XANES, and EXAFS studies, the nature of the active site was proposed as a bent mono(μ-oxo)dinickel species. The oxidation of methane to a mixture of oxygenates, methanol and formaldehyde, has also been observed for Co-ZSM-5 materials using air.[37] The product distribution was strongly dependent on the nature of the active Co center and the synthesis method conditions. Co-oxide particles (e.g., CoO, Co_3O_4) deposited by impregnation favored the formation of methanol, whereas cobalt present in ion-exchange sites favored the formation of formaldehyde. Beznis et al. were able to increase the selectivity of Co-ZSM-5 towards methanol production by altering the micro- and mesoporosity of the parent ZSM-5 material by alkaline treatments, with the aim of depositing higher loadings of Co-oxide species.[37] Zn modified zeolites, such as ZSM-5, can also activate CH_4 at low temperatures through hemolytic and heterolytic mechanisms. Xu et al. studied the room temperature activation of methane over Zn-ZSM-5 by solid-state NMR, spectroscopy studies, and DFT calculations.[38] Dinuclear Zn-oxo species were shown to favor the homolytic cleavage of the methane C-H bond, whereas, the isolated Zn^{2+} favored the heterolytic cleavage of methane. Hence, surface-bound methoxy and zinc methyl species were formed upon C-H bond activation on the two different types of active sites.

Extraction with water of the surface-bound methoxy species in Zn-ZSM-5 led to the successful formation of methanol.

2.5 Computational Chemistry

A systematic DFT study with specific treatment of Van der Waals forces has been conducted to analyze the effect of Al atom distribution within the α-ring of Zn-MFI on the activation of methane.

Computational calculations have had a remarkable evolution during the last years since these have presented an alternative to understand reaction systems. In catalysis, computational calculations have represented the understanding of different phenomena that occur on the catalyst surface and the impact of the phenomena on the reaction mechanism.[39] A selection of possible catalysts for a precise reaction can be done by studying their interactions with different species and intermediates that use computational quantum mechanics.[40] On the other hand, the optimal geometry, electronic distribution and energy, vibratory modes and thermodynamic properties of the analyzed species can be obtained by doing a quantum mechanics calculation that solve the Schrödinger equation independent of time.[41,42]

$$\hat{H}\psi_n = E_n\psi_n \tag{2.1}$$

Where $\hat{H}$ is the molecular electronic Hamiltonian operator, ψ_n the different wave functions, and E_n are the corresponding energies. The Hamiltonian operator in atomic units is given by.[43]

$$\widehat{H} = -\frac{1}{2}\sum_{i}^{electrons} \nabla_A^2 - \frac{1}{2}\sum_{A}^{nuclei} \frac{1}{M_A}\nabla_A^2 - \sum_{i}^{electrons}\sum_{A}^{nuclei} \frac{Z_A}{r_{iA}} + \sum_{i<}^{electrons}\sum_{j} \frac{1}{r_{ij}} + \sum_{A<}^{nuclei}\sum_{B} \frac{Z_A Z_B}{R_{AB}} \qquad (2.2)$$

Where ∇ is the vector differential operator, M_A is the ratio of the mass of nucleus A to the mass of an electron, Z is the nuclear change, R_{AB} is the distance between nuclei A and B, r_{ij} is the distance between electrons i and j and r_{iA} is the distance between electron I and nucleus A.[41,43]

It is possible to solve analytically the equation 2.1 for a system of an electron as the hydrogen atom. Nevertheless, when the system has two or more electrons, an analytical solution is not possible to obtain it, and several approaches are used to obtain solutions in an iterative process. The theoretical physicist, Robert Oppenheimer developed the Born-Oppenheimer Approximation. This approach consists in simplify the Schrödinger equation for molecular systems with the assumption that the nuclei does not move. It is possible to make this approach due, the nucleus movement too slow compared to the speed at which the electrons move (the speed of light), this is called Born-Oppenheimer approximation, and leads to an "electronic" Schrödinger equation.[41,43] Simplifying equation 2.2 is obtained.

$$\widehat{H} = -\frac{1}{2}\sum_{i}^{electrons} \nabla_A^2 - \frac{1}{2}\sum_{i}^{electrons}\sum_{A}^{nuclei} \frac{Z_A}{r_{iA}} + \sum_{i<}^{electrons}\sum_{j} \frac{1}{r_{ij}} \qquad (2.3)$$

For computational calculations, one approach to the treatment of electron correlation is referred to as Density Functional Theory (DFT). The method of density functional consists of expressing the electronic energy of the ground state as a function of the electron density $E_0 = E_0[\rho_0]$ where ρ_0 is a function of only the three spatial coordinates. Some of these addends consider the effect of electronic exchange and electronic correlation. In short, the density functional theory tries to calculate E_0 and other molecular properties of the fundamental state from the electron

density of this state. According to the DFT theory for a system of N-electrons, the external potential $\upsilon(r)$ is completely determined by the Hamiltonian of the system and its energy, the wave function, and other properties.[44,45] The equation $E_0 = E_0[\rho_0]$, which can be rewritten in a general way as:

$$E_0[\rho(r)] = T[\rho(r)] + \int \upsilon(r)\rho(r)dr + V_{ee}[\rho(r)] \tag{2.4}$$

Where $T[\rho(r)]$ and $V_{ee}[\rho(r)]$ are functions of the kinetic energy and the repulsion among electrons respectively. If a density $(\rho(r))$ is obtained that $\rho(r)$ is in agreement with the initial density, the operation of the energy is minimized and therefore, the energy of the system is obtained.[46-48]

2.6 References

1. Narsimhan, K.; Iyoki, K.; Dinh, K.; Román-Leshkov, Y., Catalytic Oxidation of Methane into Methanol over Copper-Exchanged Zeolites with Oxygen at Low Temperature. *ACS Central Science* **2016,** *2* (6), 424-429.
2. Bhan, A.; Iglesia, E., A Link between Reactivity and Local Structure in Acid Catalysis on Zeolites. *Accounts of Chemical Research* **2008,** *41* (4), 559-567.
3. Mango, F. D., Methane and carbon at equilibrium in source rocks. *Geochemical Transactions* **2013,** *14*, 5-5.
4. Stepanov, A. G.; Arzumanov, S. S.; Gabrienko, A. A.; Parmon, V. N.; Ivanova, I. I.; Freude, D., Significant Influence of Zn on Activation of the C-H Bonds of Small Alkanes by Brønsted Acid Sites of Zeolite. *ChemPhysChem* **2008,** *9* (17), 2559-2563.
5. Olah, G. A., Beyond oil and gas: the methanol economy. *Angew. Chem. Int. Ed.* **2005,** *44* (18), 2636-2639.
6. Olah, G. A.; Goeppert, A.; Prakash, G. K. S., Methanol and dimethyl ether as fuels and energy carriers. In *Beyond Oil and Gas: The Methanol Economy*, Wiley-VCH Verlag GmbH & Co. KGaA: 2009; pp 185-231.
7. Olah, G. A.; Goeppert, A.; Prakash, G. K. S., Fossil fuel resources and their use. In *Beyond Oil and Gas: The Methanol Economy*, Wiley-VCH Verlag GmbH & Co. KGaA: 2009; pp 29-53.
8. Hansen, J. B.; Højlund Nielsen, P. E., Methanol synthesis. In *Handbook of Heterogeneous Catalysis*, Wiley-VCH Verlag GmbH & Co. KGaA: 2008.
9. Arutyunov, V., Low-scale direct methane to methanol – Modern status and future prospects. *Catal. Today* **2013,** *215*, 243-250.
10. Balasubramanian, R.; Smith, S. M.; Rawat, S.; Yatsunyk, L. A.; Stemmler, T. L.; Rosenzweig, A. C., Oxidation of methane by a biological dicopper centre. *Nature* **2010,** *465* (7294), 115-119.
11. Rosenzweig, A. C.; Frederick, C. A.; Lippard, S. J.; Nordlund, P., Crystal structure of a bacterial non-haem iron hydroxylase that catalyses the biological oxidation of methane. *Nature* **1993,** *366* (6455), 537-543.
12. Lieberman, R. L.; Rosenzweig, A. C., Crystal structure of a membrane-bound metalloenzyme that catalyses the biological oxidation of methane. *Nature* **2005,** *434* (7030), 177-182.
13. Hakemian, A. S.; Rosenzweig, A. C., The biochemistry of methane oxidation. *Annu. Rev. Biochem.* **2007,** *76*, 223-41.
14. Hammond, C.; Conrad, S.; Hermans, I., Oxidative methane upgrading. *ChemSusChem* **2012,** *5* (9), 1668-1686.
15. Olivos-Suarez, A. I.; Szécsényi, À.; Hensen, E. J. M.; Ruiz-Martinez, J.; Pidko, E. A.; Gascon, J., Strategies for the direct catalytic valorization of methane using heterogeneous catalysis: challenges and opportunities. *ACS Catal.* **2016,** *6* (5), 2965-2981.
16. Guo, Z.; Liu, B.; Zhang, Q.; Deng, W.; Wang, Y.; Yang, Y., Recent advances in heterogeneous selective oxidation catalysis for sustainable chemistry. *Chem. Soc. Rev.* **2014,** *43* (10), 3480-3524.
17. Himes, R. A.; Barnese, K.; Karlin, K. D., One is lonely and three is a crowd: Two coppers are for methane oxidation. *Angew. Chem. Int. Ed.* **2010,** *49* (38), 6714-6716.

18. Pannov, G. I.; Sobolev, V. I.; Kharitonov, A. S., The role of iron in N_2O decomposition on ZSM-5 zeolite and reactivity of the surface oxygen formed. *J. Mol. Catal.* **1990,** *61* (1), 85-97.
19. Sobolev, V. I.; Dubkov, K. A.; Panna, O. V.; Panov, G. I., Proceedings of the second workshop on C1-C3 hydrocarbon conversion selective oxidation of methane to methanol on a Fe-ZSM-5 surface. *Catal. Today* **1995,** *24* (3), 251-252.
20. Dubkov, K. A.; Ovanesyan, N. S.; Shteinman, A. A.; Starokon, E. V.; Panov, G. I., Evolution of iron states and formation of α-sites upon activation of Fe-ZSM-5 zeolites. *J. Catal.* **2002,** *207* (2), 341-352.
21. Smeets, P. J.; Groothaert, M. H.; Schoonheydt, R. A., Cu based zeolites: a UV–vis study of the active site in the selective methane oxidation at low temperatures. *Catal. Today* **2005,** *110* (3–4), 303-309.
22. Groothaert, M. H.; Lievens, K.; van Bokhoven, J. A.; Battiston, A. A.; Weckhuysen, B. M.; Pierloot, K.; Schoonheydt, R. A., Bis(μ-oxo)dicopper as key intermediate in the catalytic decomposition of nitric oxide. *ChemPhysChem* **2003,** *4* (6), 626-630.
23. Smeets, P. J.; Groothaert, M. H.; van Teeffelen, R. M.; Leeman, H.; Hensen, E. J. M.; Schoonheydt, R. A., Direct NO and N_2O decomposition and NO-assisted N_2O decomposition over Cu-zeolites: Elucidating the influence of the Cu-Cu distance on oxygen migration. *J. Catal.* **2007,** *245* (2), 358-368.
24. Groothaert, M. H.; van Bokhoven, J. A.; Battiston, A. A.; Weckhuysen, B. M.; Schoonheydt, R. A., Bis(μ-oxo)dicopper in Cu-ZSM-5 and its role in the decomposition of NO: A combined in Situ XAFS, UV−Vis−Near-IR, and kinetic study. *J. Am. Chem. Soc.* **2003,** *125* (25), 7629-7640.
25. Woertink, J. S.; Smeets, P. J.; Groothaert, M. H.; Vance, M. A.; Sels, B. F.; Schoonheydt, R. A.; Solomon, E. I., A $[Cu_2O]^{2+}$ core in Cu-ZSM-5, the active site in the oxidation of methane to methanol. *Proc. Nat. Acad. Sci.* **2009,** *106* (45), 18908-18913.
26. Smeets, P. J.; Hadt, R. G.; Woertink, J. S.; Vanelderen, P.; Schoonheydt, R. A.; Sels, B. F.; Solomon, E. I., Oxygen precursor to the reactive intermediate in methanol synthesis by Cu-ZSM-5. *J. Am. Chem. Soc.* **2010,** *132* (42), 14736-14738.
27. Li, G.; Vassilev, P.; Sanchez-Sanchez, M.; Lercher, J. A.; Hensen, E. J. M.; Pidko, E. A., Stability and reactivity of copper oxo-clusters in ZSM-5 zeolite for selective methane oxidation to methanol. *J. Catal.* **2016,** *338*, 305-312.
28. Markovits, M. A. C.; Jentys, A.; Tromp, M.; Sanchez-Sanchez, M.; Lercher, J. A., Effect of location and distribution of Al sites in ZSM-5 on the formation of Cu-Oxo clusters active for direct conversion of methane to methanol. *Top. Catal.* **2016**, 1-10.
29. Grundner, S.; Markovits, M. A. C.; Li, G.; Tromp, M.; Pidko, E. A.; Hensen, E. J. M.; Jentys, A.; Sanchez-Sanchez, M.; Lercher, J. A., Single-site trinuclear copper oxygen clusters in mordenite for selective conversion of methane to methanol. *Nat. Commun.* **2015,** *6*.
30. Vanelderen, P.; Snyder, B. E. R.; Tsai, M.; Hadt, R. G.; Vancauwenbergh, J.; Coussens, O.; Schoonheydt, R. A.; Sels, B. F.; Solomon, E. I., Spectroscopic definition of the copper active sites in mordenite: selective methane oxidation. *J. Am. Chem. Soc.* **2015,** *137* (19), 6383-6392.
31. Zhao, Z.; Kulkarni, A.; Vilella, L.; Nørskov, J. K.; Studt, F., Theoretical insights into the selective oxidation of methane to methanol in copper-exchanged mordenite. *ACS Catal.* **2016,** *6* (6), 3760-3766.
32. Grundner, S.; Luo, W.; Sanchez-Sanchez, M.; Lercher, J. A., Synthesis of single-site copper catalysts for methane partial oxidation. *Chem. Commun.* **2016,** *52* (12), 2553-2556.

33. Wulfers, M. J.; Teketel, S.; Ipek, B.; Lobo, R. F., Conversion of methane to methanol on copper-containing small-pore zeolites and zeotypes. *Chem. Commun.* **2015,** *51* (21), 4447-4450.
34. Kulkarni, A. R.; Zhao, Z.; Siahrostami, S.; Nørskov, J. K.; Studt, F., Monocopper active site for partial methane oxidation in Cu-exchanged 8MR zeolites. *ACS Catal.* **2016**, 6531-6536.
35. Shan, J.; Huang, W.; Nguyen, L.; Yu, Y.; Zhang, S.; Li, Y.; Frenkel, A. I.; Tao, F., Conversion of methane to methanol with a bent mono(μ-oxo)dinickel anchored on the internal surfaces of micropores. *Langmuir* **2014,** *30* (28), 8558-8569.
36. Beznis, N. V.; Weckhuysen, B. M.; Bitter, J. H., Partial oxidation of methane over Co-ZSM-5: Tuning the oxygenate selectivity by altering the preparation route. *Catal. Lett.* **2010,** *136* (1), 52-56.
37. Beznis, N. V.; van Laak, A. N. C.; Weckhuysen, B. M.; Bitter, J. H., Oxidation of methane to methanol and formaldehyde over Co–ZSM-5 molecular sieves: Tuning the reactivity and selectivity by alkaline and acid treatments of the zeolite ZSM-5 agglomerates. *Microporous and Mesoporous Mater.* **2011,** *138* (1–3), 176-183.
38. Xu, J.; Zheng, A.; Wang, X.; Qi, G.; Su, J.; Du, J.; Gan, Z.; Wu, J.; Wang, W.; Deng, F., Room temperature activation of methane over Zn modified H-ZSM-5 zeolites: Insight from solid-state NMR and theoretical calculations. *Chem. Sci.* **2012,** *3* (10), 2932-2940.
39. Yates, J. T.; Johnson, J. K. *Molecular Physical Chemistry for Engineers*; University Science Books, 2007.
40. Giustino, F. *Materials Modelling Using Density Functional Theory: Properties and Predictions*; OUP Oxford, 2014.
41. Jensen, F. *Introduction to Computational Chemistry*; Wiley, 2007.
42. Dykstra, C.; Frenking, G.; Kim, K.; Scuseria, G. *Theory and Applications of Computational Chemistry: The First Forty Years*; Elsevier Science, 2011.
43. Hehre, W. J. *A Guide to Molecular Mechanics and Quantum Chemical Calculations*; Wavefunction, 2003.
44. Kenny B. Lipkowitz, D. B. B. *Reviews in Computational Chemistry*; 2007.
45. Politzer, P.; Seminario, J. M. *Modern Density Functional Theory: A Tool For Chemistry*; Theoretical and Computational Chemistry; Elsevier Science, 1995.
46. Sousa, S. F.; Fernandes, P. A.; Ramos, M. J. General Performance of Density Functionals. *J. Phys. Chem. A* **2007**, *111* (42), 10439–10452.
47. Leach, A. R. *Molecular Modelling: Principles and Applications*; Prentice Hall, 2001.
48. Frenkel, D.; Smit, B. *Understanding Molecular Simulation: From Algorithms to Applications*; Computational science series; Elsevier Science, 2001.

Chapter 3. Research objectives

The main goal of this research is to use DFT methods with long-range corrections to understand the underlying mechanism for H-atom abstraction from methane within the pores of Zn-exchanged MFI zeolite, Zn-MFI, as a function of aluminum atom positions within the α-ring. The aim of this project is to determine the properties of Zn-MFI that minimize the activation energy of C-H bond, which is the limiting step for the methanol production from methane.

The specific objectives of this work include:

- Determine the energetically favorable ion-exchange positions of Zn^{2+} as a function of aluminum atom positions within the α-ring of MFI.
- Determine the influence of aluminum atom position and Zn location on the activation energy barrier for methane C-H bond activation.
- Determine the effect of aluminum location in the α-ring on the electrostatic and electron transfer interactions of the zeolite ring on the active site.

Chapter 4. Methods

Methane activation was analyzed on zeolite MFI by creating a cluster based on the crystallography data available in the Database of Zeolite Structures.[1] The ring analyzed for aluminum substitution and metal exchange was the α-ring of MFI, which is shown in Fig. 4.1a. This ring was chosen based on previous work by Van Santeen et al. suggesting the α-ring as the most reactive location in Zn-MFI.[2-3] The α-ring of MFI is composed of seven silicon atoms, and each silicon atom exhibits a different crystallographic T-site. The crystallographic T-sites identified for the α-ring and the cluster employed in the calculations are shown in Fig. 4.1b.

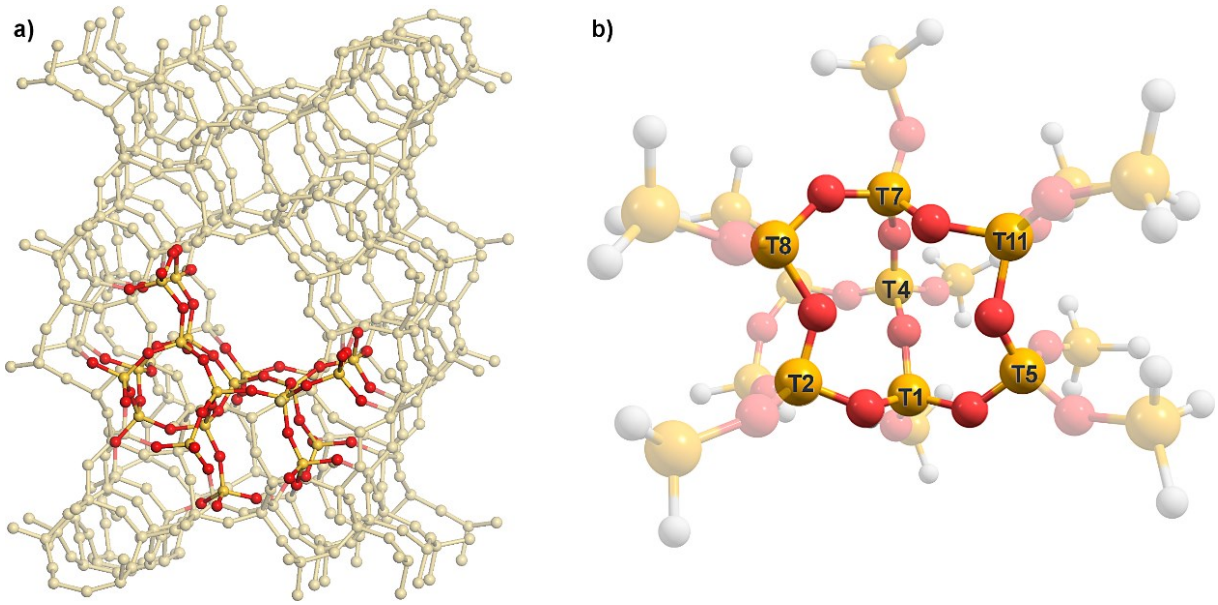

Fig 4.1. (a) MFI zeolite framework. The α-ring of the zeolite framework is highlighted with yellow for silicon atoms and red for oxygen atoms. (b) 74-atom cluster of the α-ring of MFI used in our calculations with the corresponding crystallographic T-sites identified. Hydrogen atoms are shown in white.

The substituted $ZnAl_2Si_{17}O_{22}H_{32}$ cluster analyzed in this work is composed of 74 atoms. The cluster was constructed by cutting the periodic structure, while the boundary silicon atoms were saturated with hydrogen atoms. These hydrogen atoms were aligned along the same direction of the oxygen atoms that were removed, and the Si−H bond lengths were set to 1.50 Å. Two Al atoms were substituted within the α-ring to stabilize the Zn^{2+} atom charge on the cluster.[4] As shown in Fig. 4.2, this results in 13 different configurations. All geometrical optimizations were performed on neutral charge clusters with singlet spin state.

All calculations conducted in this work used the ωB97XD as the exchange-correlation functional, which is a long-range corrected functional.[3] The basis set LANL2DZ[5] was used for the Zn atom, while 6-31+g**[6] was used for Al, O, Si, H, and C atoms. In all geometry optimization, atoms within the cluster were relaxed, except for the terminal H-atoms that were kept fixed. The partial atomic charges were obtained with the natural bond orbital (NBO) population analysis.[7] Vibrational frequencies were calculated for each optimized structure, within the rigid-rotor, harmonic-oscillator approximation. All the transition states were verified by displaying only one imaginary frequency along the reaction coordinate. All calculations were performed with Gaussian 09.[8]

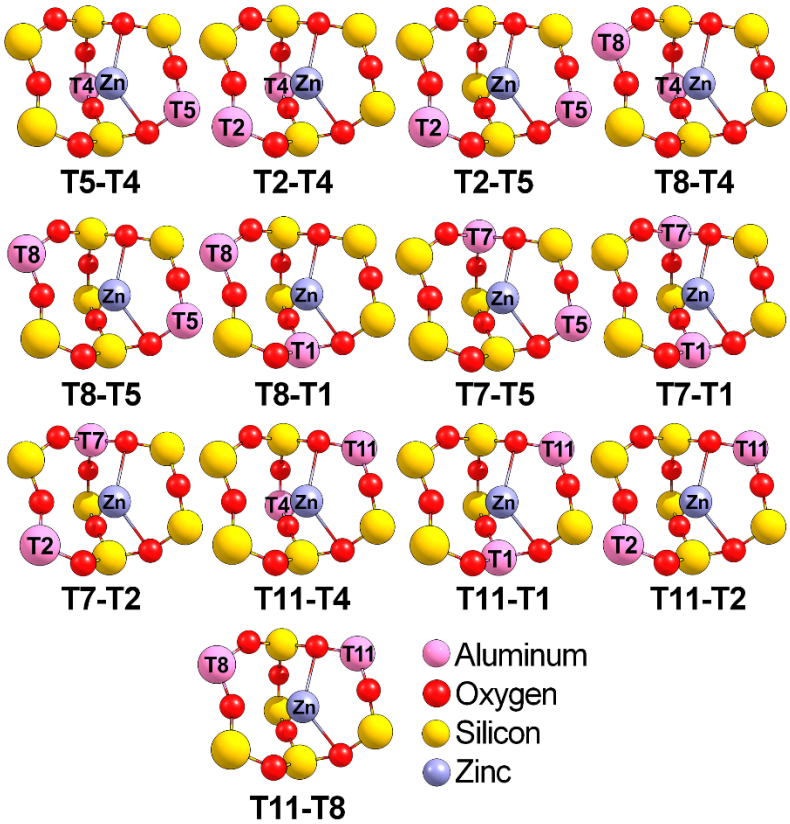

Fig 4.2 Representation of the 13 Al configurations of the α-ring. Atoms beyond the α-ring were removed from the figures for clarity.

References

1. McCusker, C. B. a. L. B. Database of Zeolite Structures:. http://www.iza-structure.org/databases/.
2. Van Santen, R. A.; Zhidomirov, G. M.; Shubin, A. A.; Yakovlev, A. L.; Barbosa, L. A. M. M., Reactivity Theory of Zinc Cation Species in Zeolites. In *Catalysis by Unique Metal Ion Structures in Solid Matrices: From Science to Application*, Centi, G.; Wichterlová, B.; Bell, A. T., Eds. Springer Netherlands: Dordrecht, 2001; pp 187-204.
3. Shubin, A. A.; Zhidomirov, G. M.; Yakovlev, A. L.; van Santen, R. A., Comparative Quantum Chemical Study of Stabilization Energies of Zn^{2+} Ions in Different Zeolite Structures. *The Journal of Physical Chemistry B* **2001,** *105* (21), 4928-4935.
4. Lowenstein, W., The distribution of Aluminium in the tetrahedra of silicates and aluminates. *American Mineralogist* **1954,** *39*, 92-96.
5. Dunning, T. H.; Hay, P. J., Gaussian Basis Sets for Molecular Calculations. In *Methods of Electronic Structure Theory*, Schaefer, H. F., Ed. Springer US: Boston, MA, 1977; pp 1-27.
6. Frisch, M. J. P., John A.; Binkley, J. Stephen, Self-consistent molecular orbital methods 25. Supplementary functions for Gaussian basis sets. *The Journal of Chemical Physics* **1984,** *80* (7), 3265-3269.
7. Foster, J. P.; Weinhold, F., Natural hybrid orbitals. *Journal of the American Chemical Society* **1980,** *102* (24), 7211-7218.
8. Frisch, M. J.; Trucks, G. W.; Schlegel, H. B.; Scuseria, G. E.; Robb, M. A.; Cheeseman, J. R.; Scalmani, G.; Barone, V.; Petersson, G. A.; Nakatsuji, H.; Li, X.; Caricato, M.; Marenich, A. V.; Bloino, J.; Janesko, B. G.; Gomperts, R.; Mennucci, B.; Hratchian, H. P.; Ortiz, J. V.; Izmaylov, A. F.; Sonnenberg, J. L.; Williams; Ding, F.; Lipparini, F.; Egidi, F.; Goings, J.; Peng, B.; Petrone, A.; Henderson, T.; Ranasinghe, D.; Zakrzewski, V. G.; Gao, J.; Rega, N.; Zheng, G.; Liang, W.; Hada, M.; Ehara, M.; Toyota, K.; Fukuda, R.; Hasegawa, J.; Ishida, M.; Nakajima, T.; Honda, Y.; Kitao, O.; Nakai, H.; Vreven, T.; Throssell, K.; Montgomery Jr., J. A.; Peralta, J. E.; Ogliaro, F.; Bearpark, M. J.; Heyd, J. J.; Brothers, E. N.; Kudin, K. N.; Staroverov, V. N.; Keith, T. A.; Kobayashi, R.; Normand, J.; Raghavachari, K.; Rendell, A. P.; Burant, J. C.; Iyengar, S. S.; Tomasi, J.; Cossi, M.; Millam, J. M.; Klene, M.; Adamo, C.; Cammi, R.; Ochterski, J. W.; Martin, R. L.; Morokuma, K.; Farkas, O.; Foresman, J. B.; Fox, D. J. *Gaussian 16*, Wallingford, CT, 2016.

Chapter 5. Results and Discussions

5.1 Overview

In this work, we have conducted a systematic study of the effect of Al atom position within the α-ring of Zn exchanged MFI on methane activation. We have studied all possible locations of the Al atoms within the ring and their effect on the energy barrier for methane activation. Our work unravels that Al atoms distribution produces a variation in the energy barrier in the detachment of a hydrogen atom from methane. Furthermore, the most energetically stable Al configuration does not yield the lowest energy barrier for methane activation.

5.2 Determination of energetically favorable Al atom substitution and Zn location in the α-ring of MFI

The relative energies of the MFI α-ring isolated clusters and the Al atom substituted cluster in certain T-sites were determined to evaluate the most stable configurations. As shown in Fig 5.1, the T11-T2 structure is the most stable configuration for the Al atom substitution, followed by T11-T1. The most unstable cluster observed is the T5-T4 combination, and it is 113 kJ/mol higher in energy than T11-T2. By comparing the optimized geometries among the optimized α-ring clusters, we note that the Zn atom is always located at the center of the α-ring, and it is coordinated to four oxygen atoms in all configurations. The representation of the Al configurations in the α-ring studied are shown in Fig 5.2.

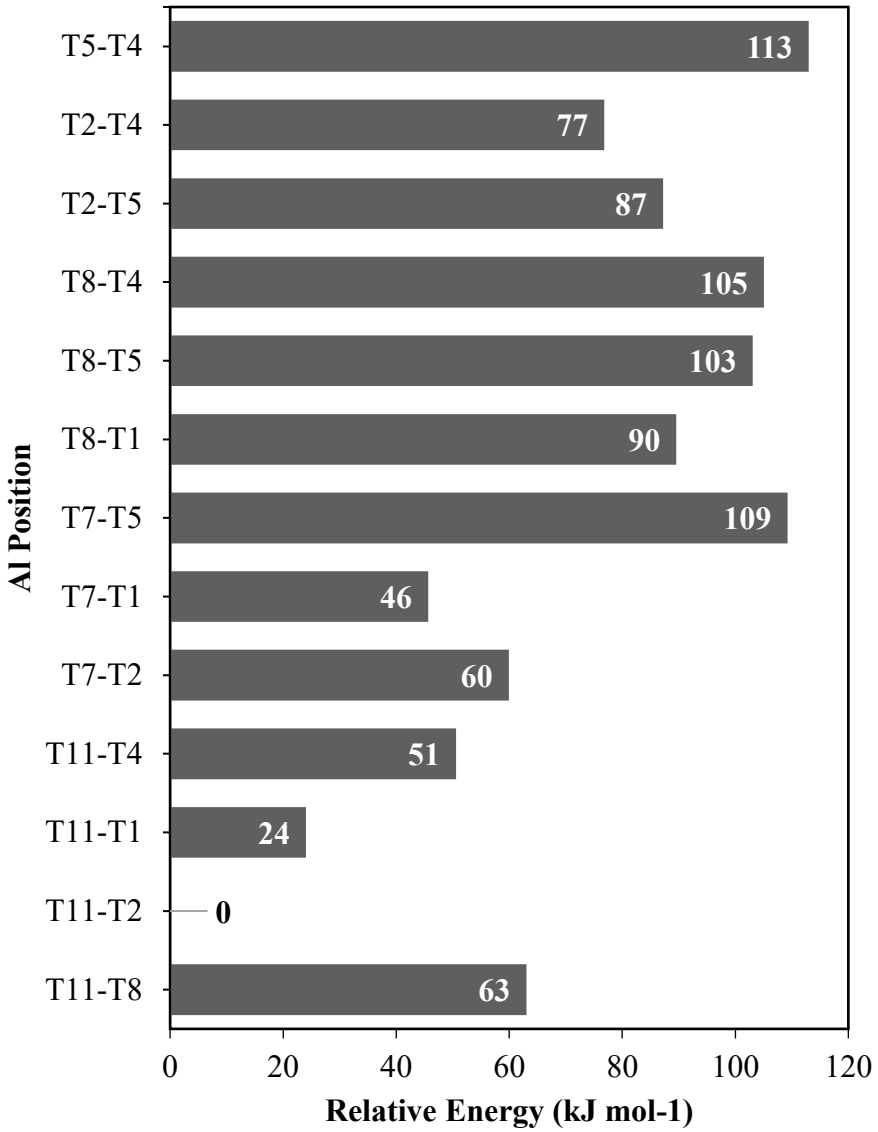

Fig. 5.1 Relative energy of the MFI α-ring cluster with respect to the lowest energy configuration, T11-T2.

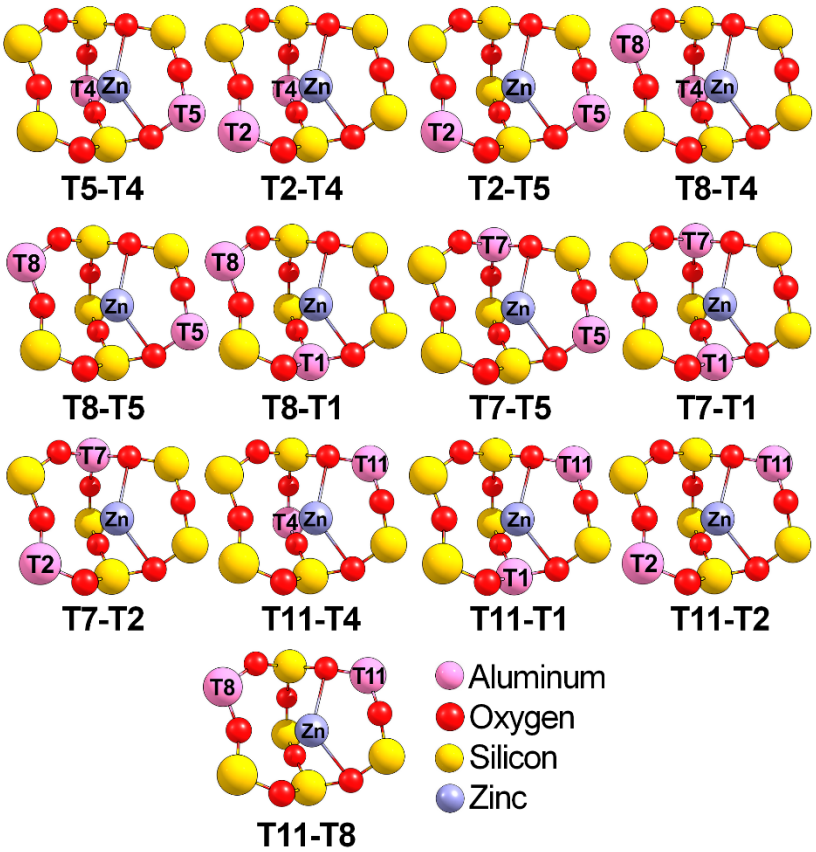

Fig. 5.2. Representation of the 13 different Al configurations of the α-ring of MFI. Atoms beyond the α-ring were removed from the figures for clarity.

In Table 4.1, the Al-Zn distances are tabulated for each cluster. These distances range from 2.75 to 3.36 Å. For the lowest energy configuration, T11-T2, the two Zn-Al distances have equal values of 2.91 Å. We also note that the O-Al-O angles formed on that configuration are similar with values of 89.2° in T11, and 91.0° in T2 site. Thus, the inclusion of the Al atoms at the T11-T2 sites yields a quasi-symmetric structure with similar distances and angles, in contrast to other configurations, in which the angles and distances parameters are not symmetric.

Table 5.1. Optimized Geometrical Parameters of the Isolated Species

Position Al_A -Al_B	***Zn-*** Al_A ***(Å)***	***Zn-*** Al_B ***(Å)***	***O1-*** Al_A***-O2*** ***(°)***	***O1-*** Al_B***-O2*** ***(°)***
T11-T8	2.87	3.25	89.46	104.60
T11-T2	2.91	2.91	89.21	91.00
T11-T1	2.89	2.70	89.36	104.96
T11-T4	2.83	3.19	90.42	103.23
T7-T2	2.98	2.91	101.62	90.99
T7-T1	2.95	2.56	97.96	92.38
T7-T5	2.75	3.28	101.08	103.83
T8-T1	3.15	2.61	98.54	95.98
T8-T5	3.36	2.99	103.49	89.12
T8-T4	3.11	2.91	104.42	95.11
T2-T5	2.91	3.25	90.35	108.96
T2-T4	2.91	3.22	92.53	102.91
T5-T4	3.18	2.90	103.35	94.06

5.3 Energetically favorable C-H bond activation in the Al substituted Zn-MFI α-ring

Methane activation involves two elementary steps: (1) methane adsorption and (2) detachment of a hydrogen atom to form methyl (CH_3) and an –OH Brønsted site. The -OH Brønsted site can be formed in any of the oxygen atoms within the α-ring or in an oxygen atom adjacent to the α-ring. It is known that the location of the –OH Brønsted site yields different reaction energies in methane activation.[1] Hence, we have systematically analyzed two plausible reaction paths for methane activation on all 13 possible Al-atom configuration of the α-ring of Zn-MFI depending on wether the Brønsted site is formed on an external oxygen atom, **Oe**, or an internal oxygen atom, **Oi**. For example, for the T8-T5 Al configuration, Fig 5.3 shows the location

of the oxygen atom where –OH Brønsted sites can be formed, we have denoted the location of oxygen atoms within the α-ring as **Oi-*n*,** where *n* is a number from one to four, and the external oxygen atoms that are located outside the α-ring as **Oe-*n***.

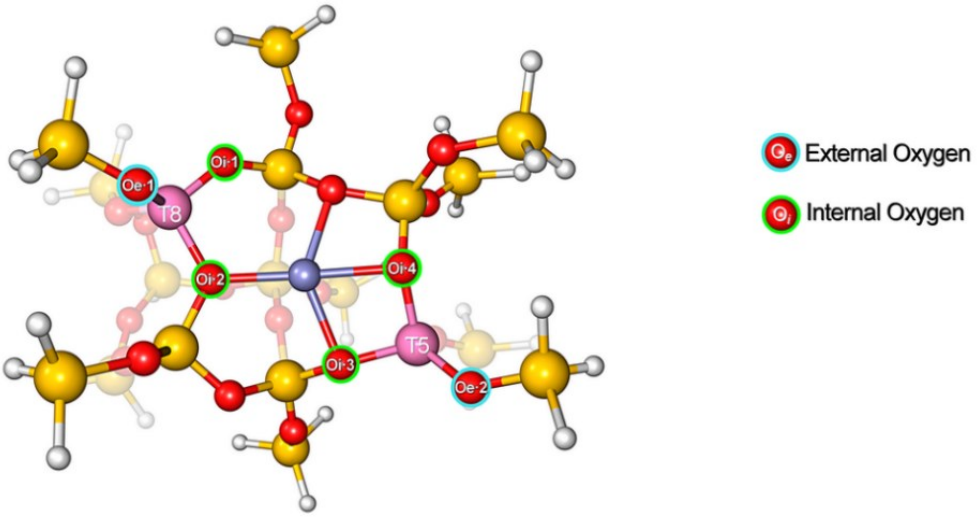

Fig. 5.3. Oxygen atoms in which the –OH Brønsted acid can be formed in the T8-T5 configuration. Oe, highlighted in light blue, denotes the oxygen atoms located outside the α-ring. Oi, highlighted in light green, denotes the oxygen atoms within the α-ring.

Once, the internal and external oxygens were identified for each cluster we analyzed two plausible methane C-H bond activation reaction paths for the 13 Al atom arrays α-ring configurations of Zn-MFI, as shown in Scheme 5.1.

Complex **I** in the mechanism shown in Fig. 5.1 corresponds to the isolated species of methane and Zn-MFI zeolite. The first step in the reaction mechanism is methane adsorption. In Complex **II**, methane is physisorbed on the zeolite. The carbon atom of methane is attracted to the positive charge of the Zn atom, but no chemical bond is formed. For all the Al substituted Zn-MFI configurations that were analyzed, methane adsorption is exothermic with minimal variations

among adsorption energies for all the Al configurations. The values of these energies vary between -36 to -48 kJ/mol corresponding to T7-T5 and T8-T5, respectively.

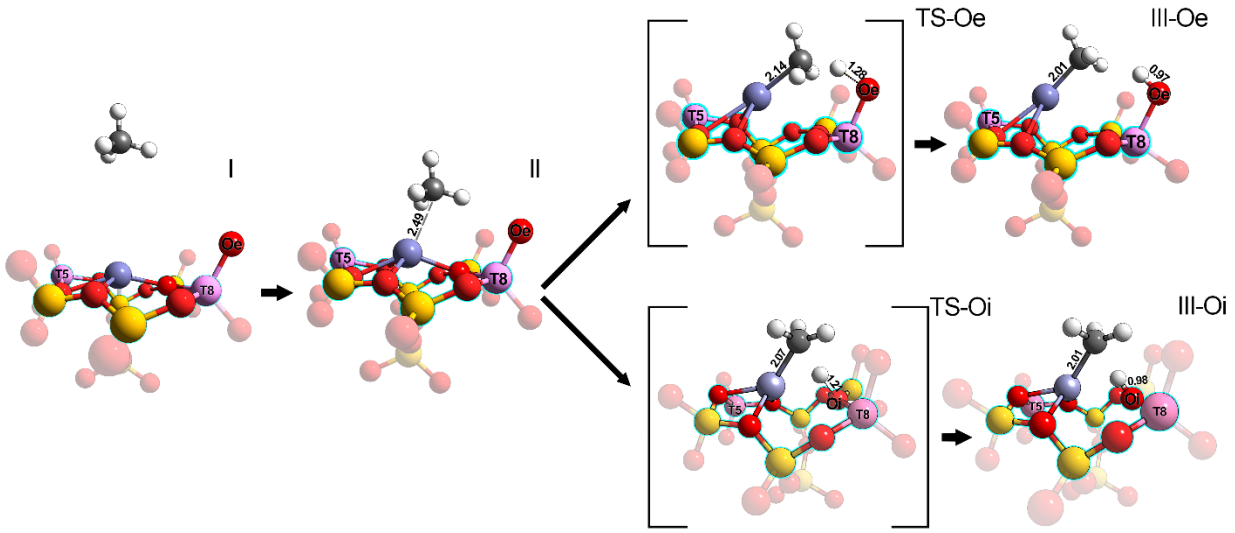

Scheme 5.1. Two reaction mechanisms studied for C-H bond activation in CH_4 in the T8-T5 Al substituted Zn-MFI α-ring. For this particular Al configuration, the most energetically favourable path involves the formation of the Brønsted acid in an external oxygen atom in the α-ring. Atoms beyond the α-ring were removed from the figures for clarity.

In contrast to the adsorption energy, the specific Al atom location has an impact on the energy for the hydrogen abstraction from CH_4. For all the Al configurations, the energies for H abstraction (complex II → complex III) are endothermic. In this step, the C atom from methane is attracted to the metal center, Zn, which results in a decrease of the distance Zn-C, from 2.46 to 2.01 Å. In this step, the hydrogen atom is transferred from methane to the oxygen atom of the zeolite framework, and the CH_3 group remains bound to the metal. For the **T8-T5** configuration, the most favorable path for the H atom abstraction from methane is the path involving an **Oe**, with an energy of 87 kJ mol^{-1}. This H atom abstraction from methane leads to the formation of the

Brønsted acid site (H-O) and methyl (CH_3). In complex **III-Oe**, the Brønsted site is formed with an **Oe** atom, whereas in complex **III-Oi** the Brønsted site is formed inside the α-ring, with an **Oi**. Figure 5.4 shows the minimum energy reaction pathways for the 13 Al configurations of the α-ring of Zn-MFI. The clusters favoring C-H bond cleavage abstraction through **Oe** are shown in Fig 5.4a, whereas clusters favoring the C-H activation through an Oi are shown in Fig 5.4b.

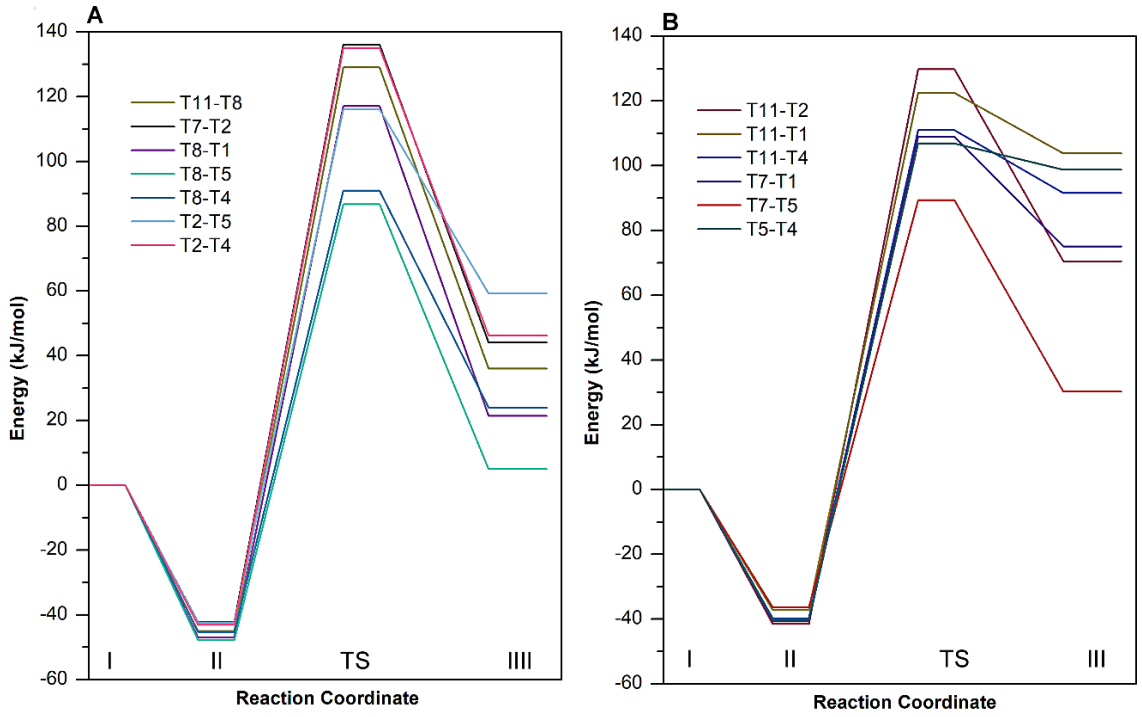

Fig. 5.4. Relative energy diagram for the extraction of a hydrogen atom from methane of all optimized structures. (I) Isolated species, (II) adsorption energy, (TS) transition state energy required to break the C-H bond and (III) Energy of the species [CH_3-Zn] and [H-O]. (**A)** Hydrogen abstraction through an **Oe** and **B**) Hydrogen abstraction through an **Oi** of the α-ring.

As shown in Fig. 5.4 a and b, the overall reaction energies for the formation of complexes **III-Oe** and **III-Oi** are different for each Al configuration. The **T8-T5** structure yields the lowest reaction energy for methane activation, with a final energy of 5 kJ/mol. The **TS** energies to form complexes **III-Oe** or **III-Oi** also vary significantly depending on the Al atom configuration

on the α-ring. **TS** energies to form **III-Oe** vary from 87 to 145 kJ/mol, and TS energies to form **III-Oi** range from 89 to 122 kJ/mol. We note that the most stable Al configuration for the isolated complex, **T11-T2**, yields an activation barrier of 145 kJ/mol, which it is the highest barrier obtained. The lowest barrier to form **III-Oi** was 89 kJ/mol on **T7-T5**, whereas the lowest barrier to form **III-Oe** was 87 kJ/mol on **T8-T5**.

5.4 Geometrical effects of the α-ring on CH_4 activation

We note that the α-ring geometrical parameters of the clusters that we analyzed are modified upon methane activation. For instance, in Complex **II**, the angle between the Al atoms and the two adjacent oxygen atoms change when compared to the isolated zeolite cluster. Additionally, the distance between the zinc and carbon atoms vary from 2.56 to 2.91 Å, as shown in Table 4.2.

Table 5.2. Optimized Geometrical Parameters of the Species Involved in the Methane Adsorption

Position Al_A -Al_B	***Zn-*** Al_A^* ***(Å)***	***Zn-*** Al_B^{**} ***(Å)***	***Zn-C (Å)***	***O1-*** Al_A***-O2*** (°)
T11-T8	2.87	3.25	2.61	89.47
T11-T2	2.91	2.91	2.58	89.62
T11-T1	2.89	2.70	2.74	89.94
T11-T4	2.83	3.19	2.74	90.88
T7-T2	2.98	2.91	2.68	91.43
T7-T1	2.95	2.56	2.72	97.01
T7-T5	2.75	3.28	2.62	102.32
T8-T1	3.15	2.61	2.61	98.54

T8-T5	3.36	2.99	2.59	103.49
T8-T4	3.11	2.91	2.91	104.11
T2-T5	2.91	3.25	2.64	108.96
T2-T4	2.91	3.22	2.61	93.32
T5-T4	3.18	2.90	2.56	95.21

The Al configurations, however, do not have a significant impact on the Zn-C bond lengths formed in complexes **III-Oi** and **III-Oe**. Thus, the Zn-C distance was shown to be independent of the location of the Brønsted site, and for all configurations, the Zn-C bond length was on average 2.01Å. This result is in good agreement with the experimental value reported by Østby and coworkers, with 2.5% error.[2] The formation of the Zn-C bond causes the Zn atom to lose a coordination with one of the O atoms within the α-ring, and this is reflected through an increase of the Zn-O distance. For instance, in the **T8-T5** Al-configuration the Zn-O distance increased from 2.11 to 3.03 Å.

5.5 Highest Occupied Molecular Orbital (HOMO) and Lowest Unoccupied Molecular Orbital LUMO orbitals

The acidity of the zeolites is of considerable importance since this directly affects the catalytic activity in the break of the C-H bond from methane. For this reason, the calculation of LUMO energy is necessary to measure the material lewis acidity, in search of finding a connection with the transition state energy, shown in Fig.5.4. Our results indicate that for a specific Al array, the lowest energy for methane activation is obtained for complexes in which the formation of the Brønsted acid site on the oxygen atom is located in the highest occupied molecular orbital (HOMO) of the isolated cluster. For instance, Figure 5.5a illustrates the HOMO orbitals for the

T8-T5 Al configuration. For this configuration, the lowest reaction energy for methane activation was obtained when the Brønsted site was located on **Oe1**. On the basis of our results, the location of the HOMO orbital can be used to identify the oxygen atom in which the formation of the Brønsted site which would yield the lowest reaction energy for methane activation. Fig 5.6 shows the HOMO and LUMO localization for all structures studied.

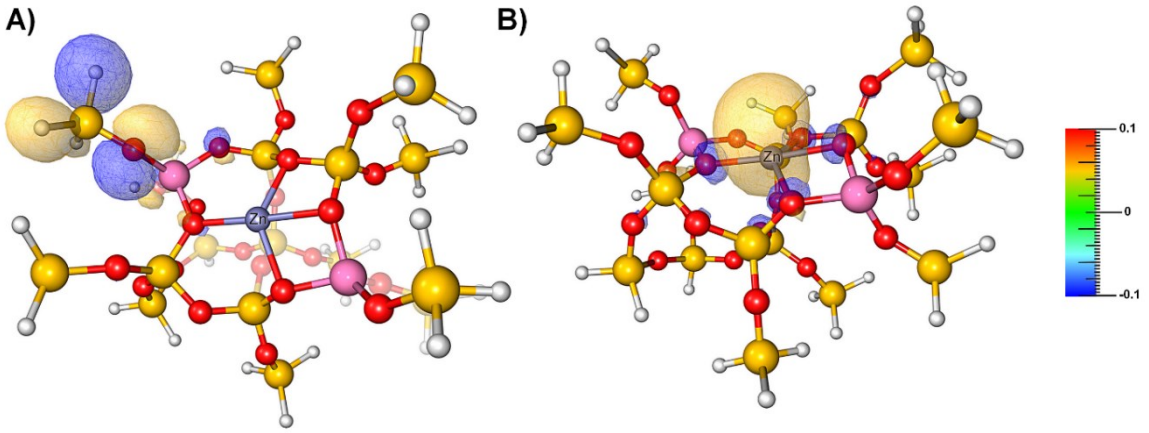

Fig 5.5 The HOMOs **(a)** and LUMOs **(b)** are shown for the T8-T5 cluster.

Positions	**HOMO**	**LUMO**
T11-T8	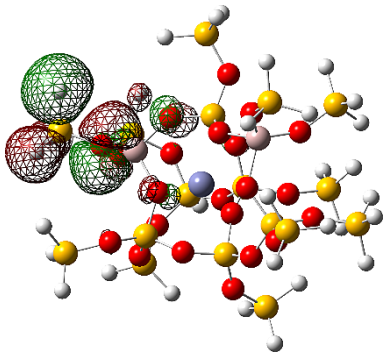	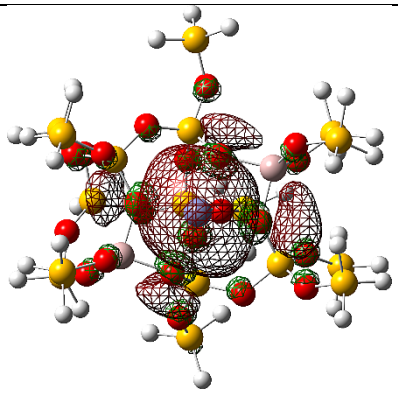

T11-T2	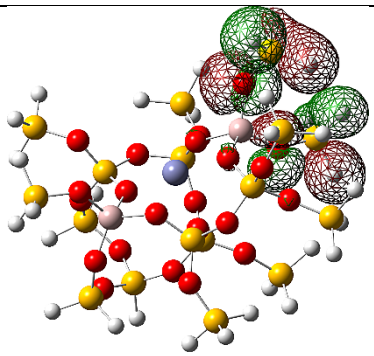	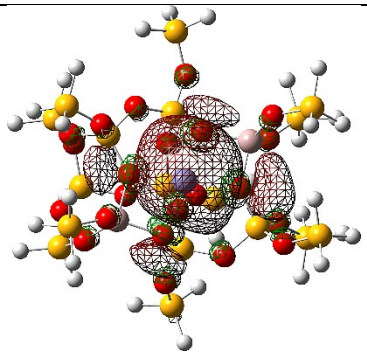
T11-T1	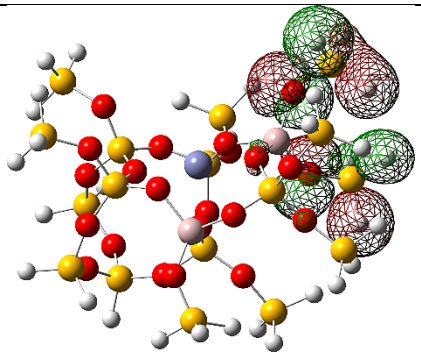	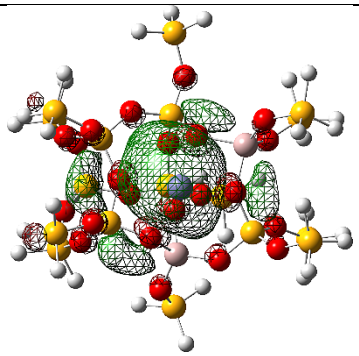
T11-T4	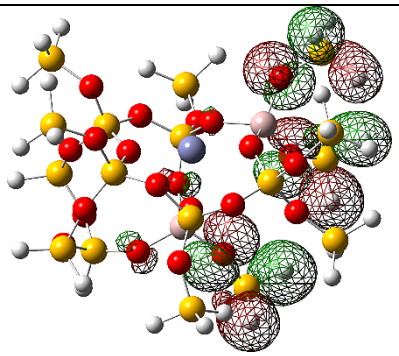	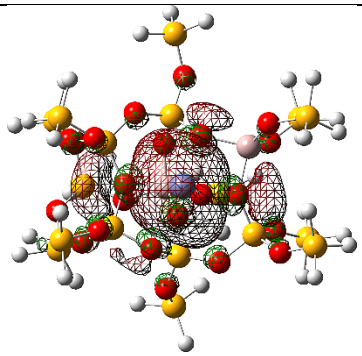
T7-T2	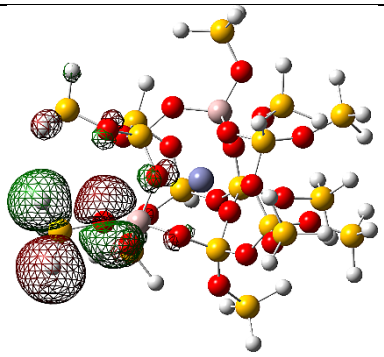	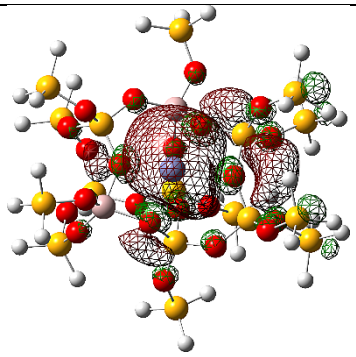

T7-TI	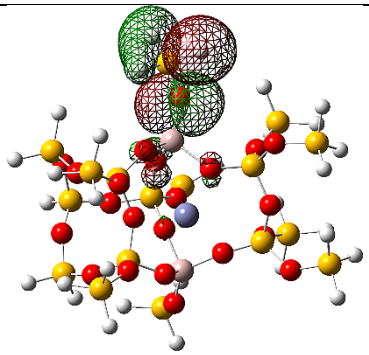	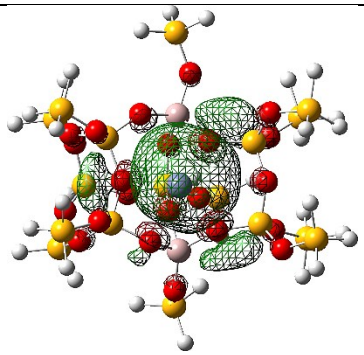
T7-T5	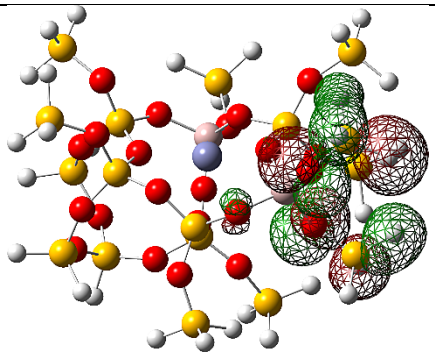	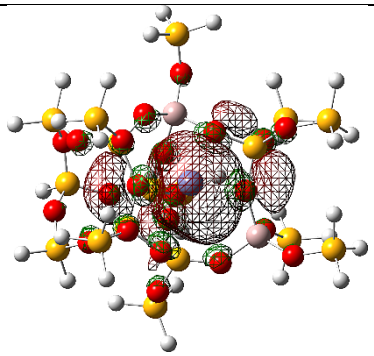
T8-T1	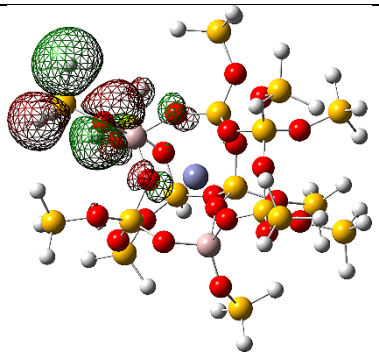	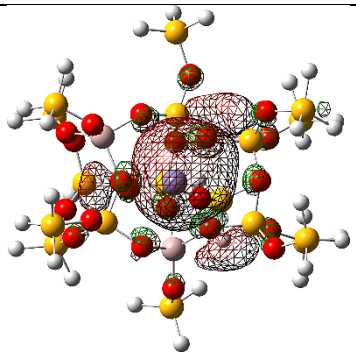
T8-T5	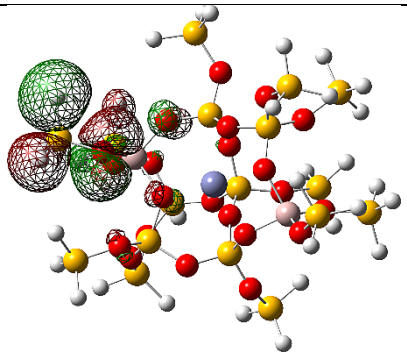	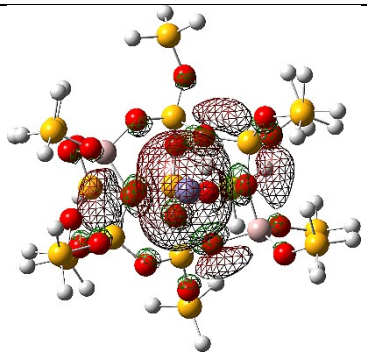

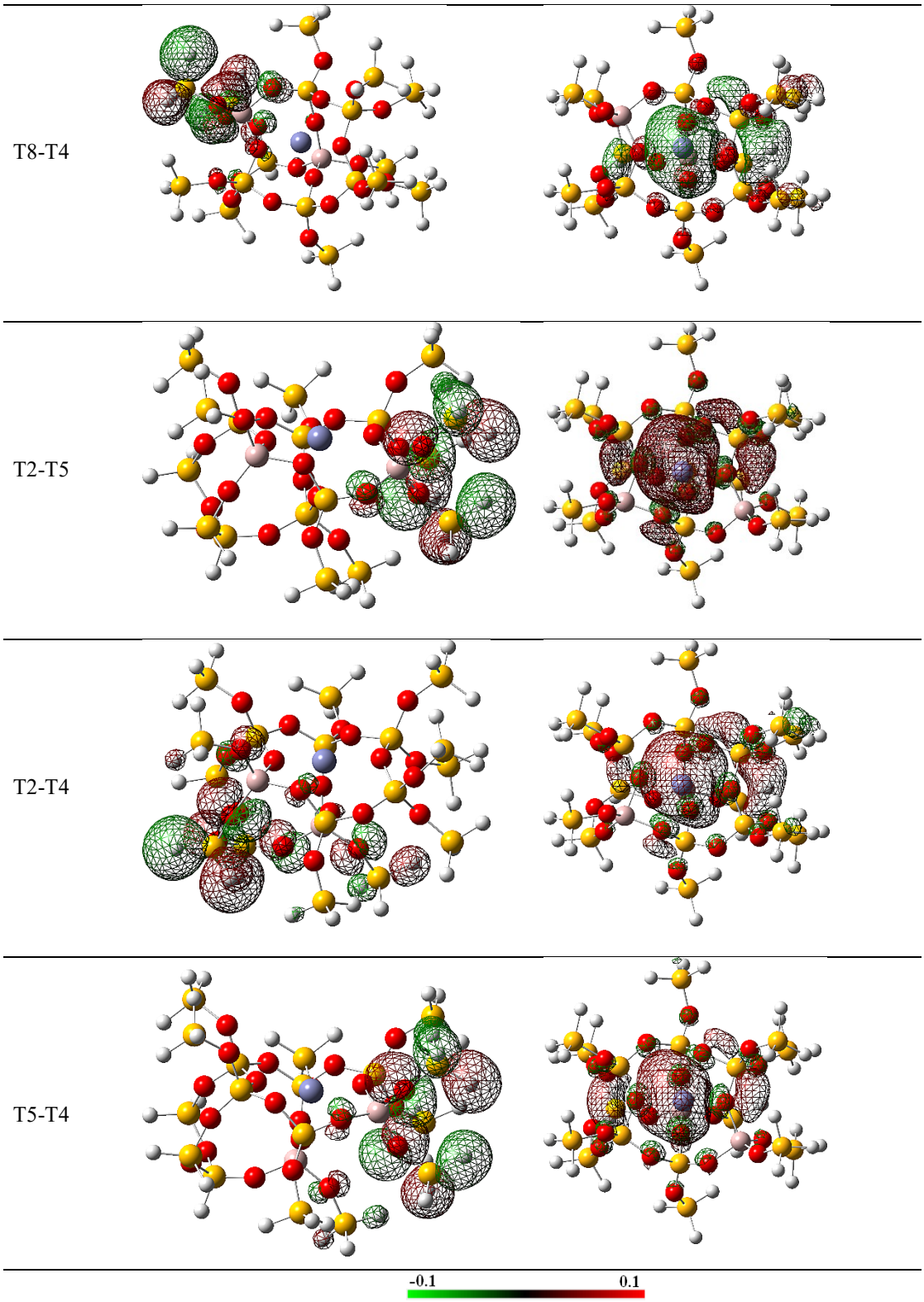

Fig 5.6. HOMO and LUMO Orbitals of Optimized Clusters.

The energies of the LUMO were also analyzed to evaluate the Lewis acidity of clusters studied. Fig 5.7 shows the relationship between the LUMO energy and the transition state energy for each of the studied arrays. Our calculations demonstrate that LUMO energies do not have a clear dependence on the Al configuration of the clusters. Nevertheless, the lowest LUMO energy corresponds to the T8-T5 Al configuration, which suggests that this specific Al configuration provides the highest Lewis acidity in this material.

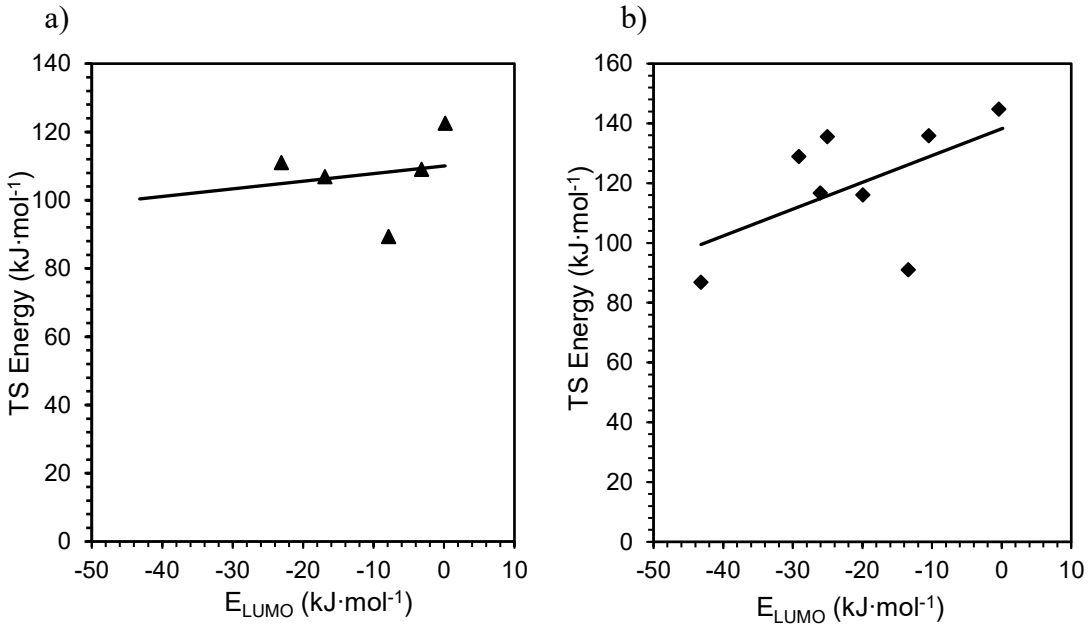

Fig 5.7. LUMO Energy vs Transition State Energy. Dependence of transition state energy on the energy of the LUMO orbital. A) Transition state energies correspond when the H atom joins an **Oi** atom (▲) and b) energies are associated to the H atom abstraction by an **Oe** atom (◆).

5.6 Effect of Zn charge (q_{Zn}) on C-H bond activation

The Al-atom distribution within the active site of Zn-MFI can also significantly affect the energy required for the abstraction of the H atom of CH_4. Thus, we further analyzed the effect of the Al array on the active site of Zn-MFI, and our calculations demonstrate that the charge of the

Zn atom (**q_{Zn}**) is affected by the position of the Al atoms within the α-ring of MFI. The **q_{Zn}** ranged from 1.57 for T5-T4 to 1.63 for T8-T5, all values obtained are shown in Table 4.3.

Our calculations further revealed that changes on **q_{Zn}** could be correlated to the energy barrier of methane C-H bond activation. Fig 5.8a shows the trends for the Al configurations in which the minimum energy path leads to the formation of complex **TS-Oi**. As shown in Fig 5.8a, for the clusters in which it is energetically favorable to form the Brønsted site within the α-ring of Zn-MFI, the energy of the transition state decreases as the charge of the Zn atom decreases. However, for the clusters in which it is favorable to form the Brønsted site outside the α-ring, the transition state energy decreases with increasing charge of the Zn atom.

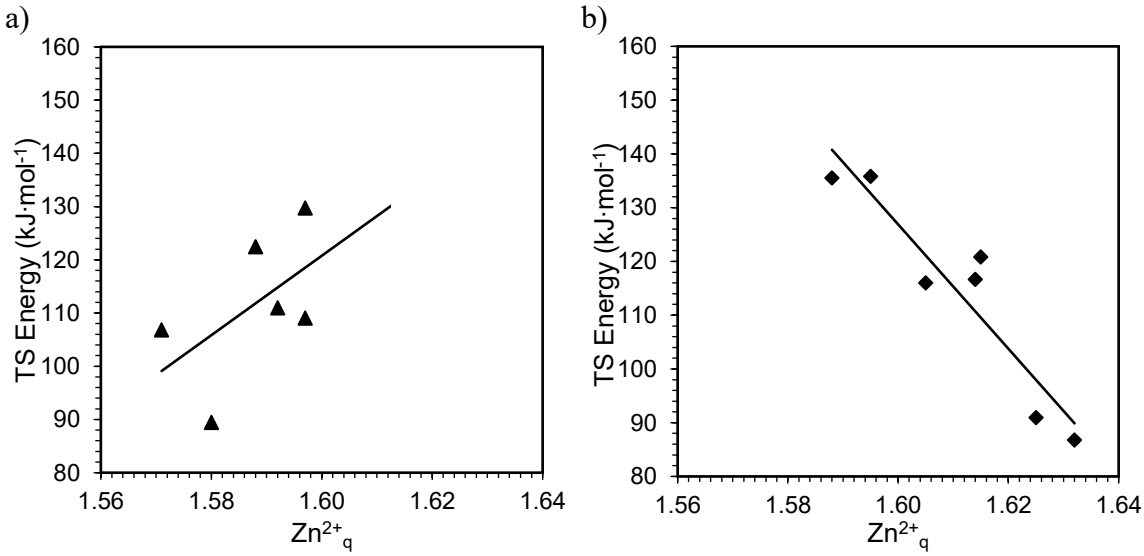

Fig 5.8. Dependence of transition state energy regarding Zn charge when the species are isolated. A) transition state energies for H atom abstraction by an **Oi** atom in the α-ring and (▲) B) transition state energies for H atom abstraction by an **Oe** atom in the α-ring (◆).

Table 5.3. The Charge of the Zinc (q_{Zn}) in the α-ring.

Position ***Al_A -Al_B***	q_{Zn}

T11-T8	1.615
T11-T2	1.600
T11-T1	1.588
T11-T4	1.592
T7-T2	1.595
T7-T1	1.597
T7-T5	1.580
T8-T1	1.614
T8-T5	1.632
T8-T4	1.625
T2-T5	1.605
T2-T4	1.588
T5-T4	1.571

5.7 References

1. Montejo-Valencia, B. D.; Pagán-Torres, Y. J.; Martínez-Iñesta, M. M.; Curet-Arana, M. C., Density Functional Theory (DFT) Study to Unravel the Catalytic Properties of M-Exchanged MFI, (M = Be, Co, Cu, Mg, Mn, Zn) for the Conversion of Methane and Carbon Dioxide to Acetic Acid. *ACS Catalysis* **2017**, *7*, 6719-6728.
2. Haaland, A. a. G., Jennifer C. and McGrady, G. Sean and Downs, Anthony J. and Gullo, Emanuel and Lyall, Mark J. and Timberlake, Jessima and Tutukin, Andrey V. and Volden, Hans Vidar and Ostby, Kari-Anne, The Length, Strength and Polarity of Metal-Carbon Bonds: Dialkylzinc Compounds Studied by Density Functional Theory Calculations{,} Gas Electron Diffraction and Photoelectron Spectroscopy. *The Royal Society of Chemistry* **2003**, 4356-4366.

Chapter 6. Conclusions

We have conducted a systematic DFT study with specific treatment of Van der Waals forces to analyze the effect of Al atom distribution within the α-ring of Zn-MFI on the activation of methane. Our results demonstrate that:

i) The most stable configuration with the lowest energy for Zn^{2+} ionic exchange is obtained when the Al atoms are located in the **T11-T2** crystallographic sites of the α-ring of MFI.

ii) The dissociative adsorption of CH_4 takes place on Zn in which the H-atom bonds to an oxygen in the framework of the α-ring in MFI.

iii) Methane adsorption on the active site of Zn is independent of the configuration of Al atoms in the α-ring.

iv) The H-atom has several sites for abstraction by oxygen in the cluster, nevertheless the lowest activation energy is observed for clusters with oxygen sites located in the HOMO.

v) Our results suggest that the partial atomic charge of the Zn atom within the α-ring of MFI can be correlated to the transition state energy of methane activation.

The fundamental studies conducted in this work contribute to the elucidation of essential parameters and correlations, based on electrostatic and electron transfer interactions, for the activation of CH_4 Zn-MFI zeolites. This work contributes to the rational design of catalytic

materials for methane activation, which can provide experimentalist with insights on the synthesis of highly active zeolite catalyst for methane activation.